Electrochemical Exfoliation of Graphene in Aqueous Media

Pushp Raj Harsh [a], Ujjwal Prasad [a], S.R. Kumar [b], Nandu B. Chaure [c], Kamal Prasad [a,*]

[a] *University Department of Physics, T.M. Bhagalpur University, Bhagalpur - 812007, India*

[b] *Department of Applied Science and Humanities, NIAMT, Hatia, Ranchi - 834003, India*

[c] *Department of Physics, Savitribai Phule Pune University, Pune - 411007, India*

Editor's note: Harsh et al. presented an efficient method for synthesizing low-defect graphene via electrochemical exfoliation in water. Applying voltage with elevated temperature (75°C) enhanced production efficiency and yielded high-quality graphene with large crystallite size, suitable for energy storage and sensors. The findings support future advancements in materials development.

doi: 10.22034/jams.2026.260207

How to cite: P.R. Harsh et al., *Journal of Applied Material Science*, **2026**, *2*, 260207.

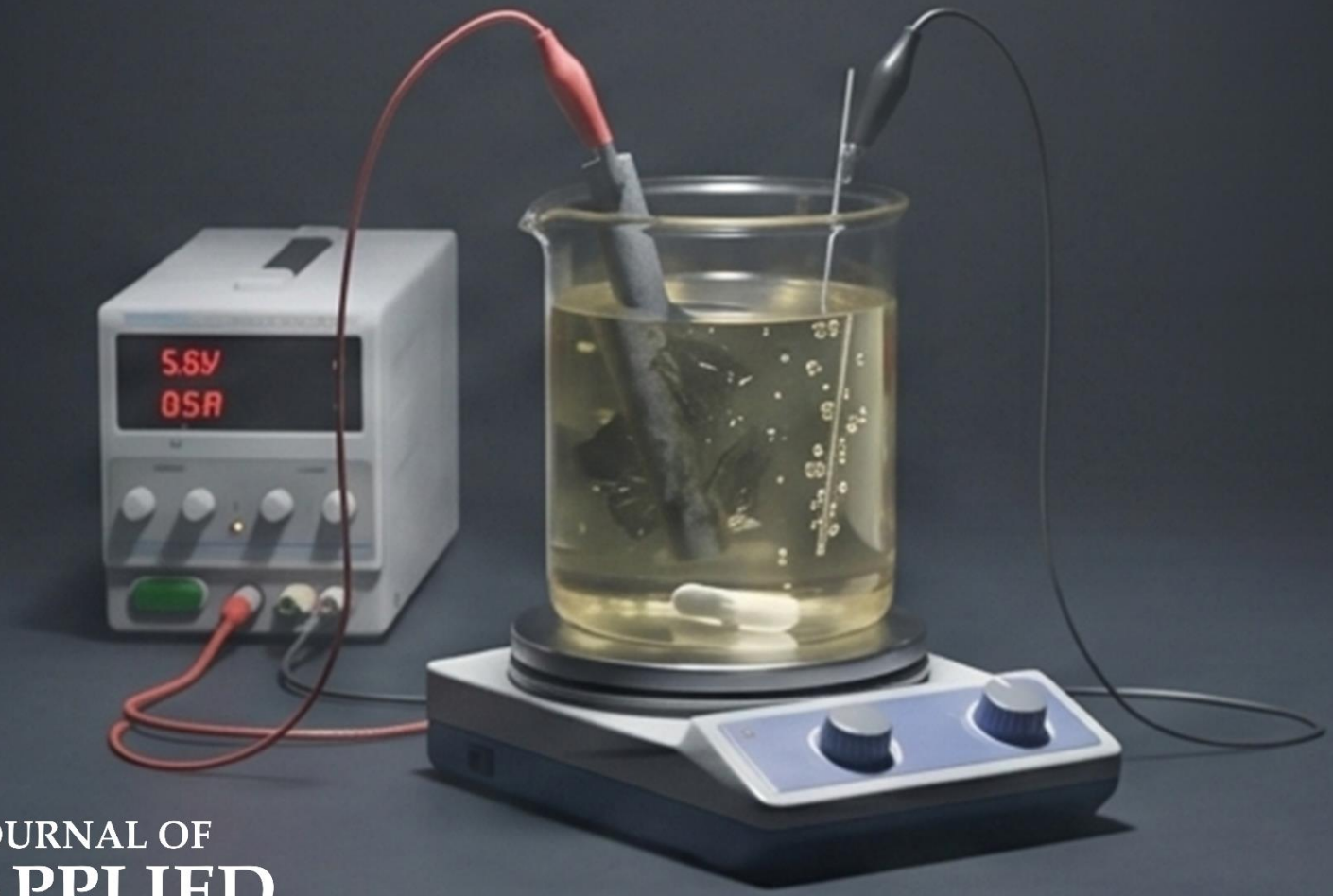

JOURNAL OF
APPLIED
MATERIAL
SCIENCE
jams.hsu.ac.ir

Journal of Applied Material Science **2026**, 2, 260207
How to cite: P.R. Harsh et al., *Journal of Applied Material Science*, **2026**, 2, 260207.
Journal homepage: **jams.hsu.ac.ir**

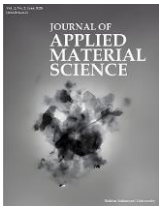

Original Research

Electrochemical Exfoliation of Graphene in Aqueous Media

Pushp Raj Harsh [a], Ujjwal Prasad [a], S.R. Kumar [b], Nandu B. Chaure [c], Kamal Prasad [a,*]

[a] *University Department of Physics, T.M. Bhagalpur University, Bhagalpur - 812007, India*

[b] *Department of Applied Science and Humanities, NIAMT, Hatia, Ranchi - 834003, India*

[c] *Department of Physics, Savitribai Phule Pune University, Pune - 411007, India*

Abstract

The current study presents a promising bulk approach to synthesizing low-defect graphene using the electrochemical exfoliation technique in an aqueous medium, where an applied voltage generates SO_4^{2-} ions that intercalate between the stacked graphite layers, forming gaseous species that broaden the interlayer spacing and exfoliate graphene sheets. Additionally, the incorporation of an elevated temperature of 75°C further intensifies the reaction rate, which enhances the production efficiency and reduces the overall latency. This method presents a simple and environmentally sustainable approach for graphene synthesis, highlighting its potential for green chemistry applications. Characterizations like XRD, Raman spectroscopy, SEM, EDS, TEM, and UV-Visible studies confirm the formation of good-quality graphene, accompanied by the least number of layers of graphene. Our findings demonstrate a high production yield and noticeably large crystallite size, which makes it a great contender for energy storage and sensor applications. This study provides valuable insights into advanced materials synthesis, laying the groundwork for future research and the development of applications-oriented technologies.

Keywords: Electrochemical exfoliation; Graphene; Raman spectroscopy; UV-visible spectroscopy; Optical property.

1. Introduction

Graphene represents the essential two-dimensional (2D) structure unit underlying all sp^2 hybridized carbon allotropes. When stacked in horizontally parallel arrangements, graphene sheets give rise to three-dimensional (3D) graphite, which can be transformed into one-dimensional (1D) carbon nanotubes through rolling or zero-dimensional (0D) fullerenes [1]. Owing to their remarkable physicochemical characteristics, graphene and its derivatives have positioned them at the forefront of numerous high-performance cutting-edge technological innovations. These encompass low-density, flexible, thin, and long-lasting screens and electronically run circuits; high-performance supercapacitors [2], field-effect transistors [3],

* Corresponding author.
Email address: prasad_k@tmbuniv.ac.in (K. Prasad)

Received 2 February 2026
Revised 19 April 2026
Accepted 2 May 2026
Available online 19 May 2026

https://doi.org/10.22034/jams.2026.260207

transparent conductive electrodes as an alternative to indium tin oxide (ITO); conductive polymer composite [4], extensive surface area nano-material for efficient energy storage technologies [5], and photovoltaic units, particularly solar cells [6], etc.

Distinguished members of the graphene family have emerged as key candidates for industrial scale-up applications, particularly as high-value additives and functional fillers. Among existing synthesis processes, mechanical exfoliation [7] yields pristine graphene but suffers from low throughput and limited flake size, limiting its suitability for large-scale production. Chemical Vapor deposition (CVD) [8, 9] enables large area graphene film with controlled thickness, but requires high temperature and reactive gases, limiting its scalability. Epitaxial growth [10] produces high-quality graphene, though with small flake sizes and high energy demands. Chemical oxidation methods offer a scalable route for bulk graphene-based materials [11]. Traditional approaches like Hummer's [12] methods release toxic gases, posing environmental risks. Despite extensive research into diverse graphene synthesis techniques, the scalable fabrication of superior-grade graphene from natural graphite remains a persistent technical obstacle.

This study aims to explore the feasibility of utilizing a graphite electrode as a cost-effective and readily available precursor to exfoliate premium quality graphene via an electrochemical route. Exfoliation through the electrochemical route, nowadays, has garnered significant recognition owing to its operational accessibility, rapid processing time, and its capacity to yield a premium class of graphene along with desirable structural and electrical characteristics. It is known that the electrochemical exfoliation of graphite can be engineered through anodic or cathodic approaches. In cathodic exfoliation, positively charged ions intercalate, whereas in anodic exfoliation, negatively charged ions are driven toward the graphite electrode. The generated reactive species promote oxidative attack on the graphite lattice, resulting in progressive structural deterioration and a consequent decline in graphene quality.

Conversely, cathodic exfoliation proceeds under reductive conditions induced by an applied negative potential, effectively suppressing the formation of oxidative intermediates [13]. A further advancement was reported by Zhang et al., who developed a sandwich-structured graphite electrode configuration capable of operating simultaneously as both the anode and the cathode [14]. In our study, anodic exfoliation was employed, where SO_4^{2-} ions from $FeSO_4$ electrolyte intercalate between graphite layers. This intercalation expands the d-spacing, weakening the van der Waals interactions. Upon the application of an anodic potential, the intercalated sulfate ions are partially decomposed into gaseous products (SO_2, O_2, H_2), generating internal pressure that facilitates rapid exfoliation.

Anodic exfoliation is further enhanced by the formation of hydroxyl and oxygen-containing radicals at the electrode–electrolyte interface. These reactive species selectively attack intrinsic defects and edges, thereby assisting delamination. However, excessively slow exfoliation may lead to unwanted oxidation and hydrophilic graphene formation. To avoid this, fast exfoliation is preferred, which is promoted by both the electrolyte chemistry and operating temperature. Elevated electrolyte temperature has been shown to accelerate exfoliation kinetics. For example, Tripathi et al. [15] demonstrated that increasing electrolyte temperature to 80°C enhanced yield by a factor of 4.5. Heating enhances ion vibration, promotes interlayer expansion, reduces defect density, and results in larger lateral graphene sheets. In the present case, the combined use of $FeSO_4$ electrolyte and elevated temperature provides a synergistic effect: Fe^{2+} acts as a redox buffer to limit excessive oxidation, while SO_4^{2-} ensures efficient intercalation and gas-assisted exfoliation. The higher temperature reduces production time, increases yield, and improves graphene quality by producing multilayer graphene with fewer defects and larger flake sizes. While acidic electrolytes (such as H_2SO_4) can produce graphene with larger sheet sizes and good quality, they often cause over-oxidation, introducing excess oxygen groups, which hamper the many intriguing properties of graphene.

Zhou et al. [16] attempted to address this by using sodium dodecyl sulphate and thionin acetate to obtain few-layer graphene. However, such methods still rely on hazardous chemicals and harsh ionic liquids, involve extra processing steps, and frequently result in low-quality multilayer graphene. Studies have shown that the presence of SO_4^{2-} in electrolytes significantly enhances the efficiency of the electrochemical exfoliation process, facilitating more effective intercalation and subsequent delamination of the graphite layer. In the anodic exfoliation, ions having a negative charge, like SO_4^{2-}, intercalate into graphite layers, driven by the

applied potential. These ions, along with co-intercalating species, disrupt van der Waals forces through electrochemical reactions, leading to layer separation. Process parameters such as voltage, current, duration, and electrolyte composition were optimized to control the graphene's defect density, oxygen content, number of layers, and lateral size.

A Critical comparison with previously reported electrochemical exfoliation strategies further underscores the distinguishing features of the present work. Strong acidic electrolytes such as H_2SO_4 have been widely employed for anodic exfoliation; however, these systems typically operate under highly oxidative conditions, often leading to increased defect density and limited structural control. For instance, graphene synthesized in 0.1 M H_2SO_4 under anodic conditions (with pulse sonication) has been reported to exhibit an I_D/I_G ratio of ~1.18, indicating a relatively higher degree of disorder [17]. Neutral sulfate-based electrolytes such as $(NH_4)_2SO_4$ have also been explored, often in combination with additives or auxiliary treatments.

Studies such as Zhao et al. [18] and Raj et al. [17] demonstrate improved exfoliation efficiency; however, these approaches involve additional processing steps and frequently result in higher defect densities (I_D/I_G ratio of ~0.92-2.08), reflecting a trade-off between process efficiency and material quality. Moreover, the present study employs $FeSO_4$ as a single electrolyte under moderately elevated temperature (75°C) in a simplified two-electrode configuration. Under optimized conditions, the production yield increased from ~117 mg to ~206 mg, accompanied by a reduction in exfoliation time, indicating enhanced process efficiency. The resulting graphene exhibits a comparatively lower defect density and a smaller number of layers, demonstrating improved structural preservation relative to many previously reported systems. The electrochemically exfoliated graphene sample was characterized using X-ray diffraction (XRD), Raman spectroscopy, scanning electron microscope (SEM), energy dispersive X-ray analysis (EDS), transmission electron microscope (TEM), and UV-Visible studies.

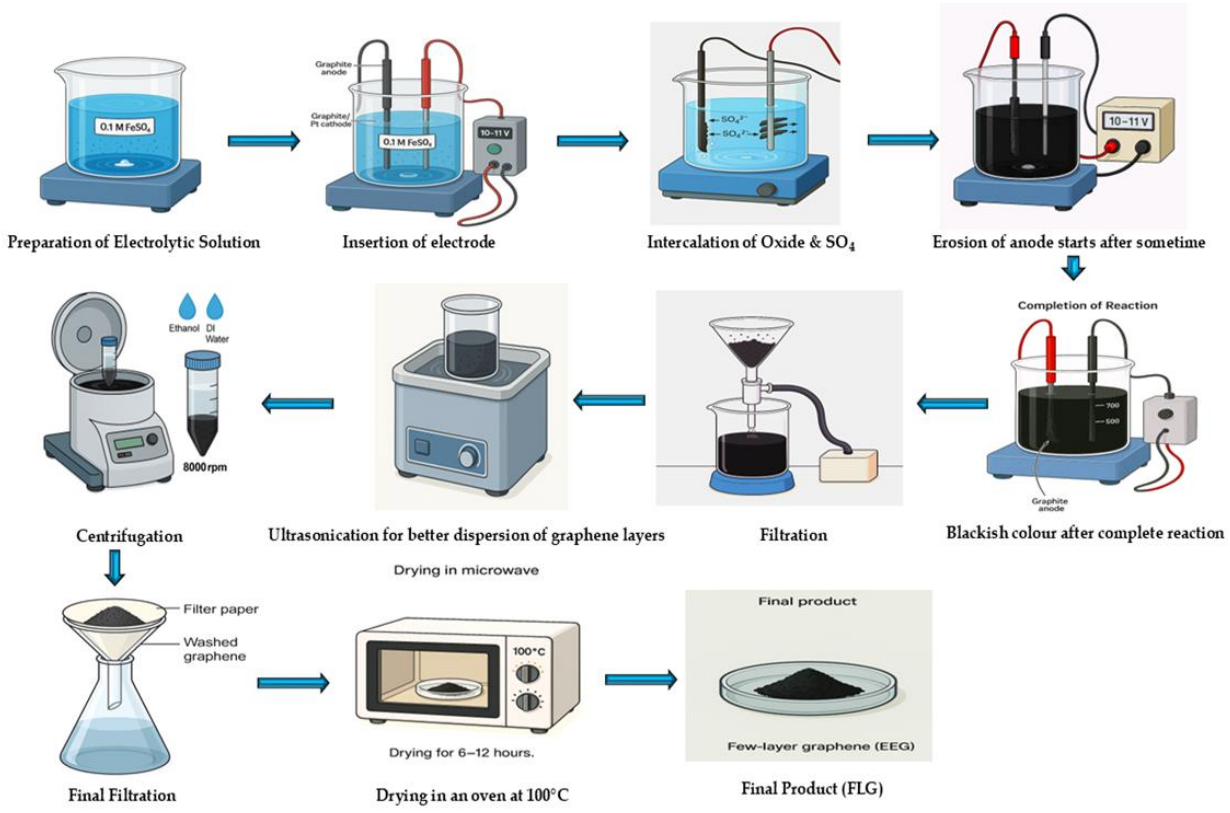

Figure 1. Schematic diagram for the preparation of electrochemically exfoliated graphene.

2. Experimental

2.1. Materials

Graphite Electrode (HOPG): A highly oriented pyrolytic graphite (HOPG) electrode with a density of 1.5 g cm^{-3} and purity of 99.9% (analytical reagent, AR, grade) was procured from Nanoshel. Ferrous Sulfate Heptahydrate ($FeSO_4 \cdot 7H_2O$): AR-grade $FeSO_4 \cdot 7H_2O$ with 99.9% purity was purchased from Sigma-Aldrich.

2.2. Sample preparation

Figure 1 illustrates the schematic diagram, experimental setup, electrolytic solution after complete reaction, anodic electrode after reaction, and the exfoliated graphene. In this study, graphene was extracted electrochemically from a graphite electrode in an aqueous environment using a two-electrode system. In the two-electrode configuration, graphite rods were functioning as both anode and cathode. An aqueous electrolyte was formulated by dissolving 0.1 M Iron (II) sulfate ($FeSO_4$) (AR grade) in 45 ml of distilled water, with continuous magnetic stirring for 15 minutes at ambient temperature. After that, we maintain the electrolyte temperature of 75°C for the rest of the procedure. Both graphite electrodes were submerged in the prepared electrolytic solution, maintaining an inter-electrode spacing of 2 cm. A constant 14 V DC potential was applied using a HM5041 power supply. After 35 minutes of applying the potential and heat, exfoliation of the graphite anode was initiated, resulting in the formation of blackish colored precipitate near the base of the electrolytic solution. The process continued for 4 hours, during which a homogeneous electrolytic solution was formed. After the complete electrochemical exfoliation, the obtained product was thoroughly rinsed with double-distilled water and ethanol using centrifugation to ensure the removal of any ferrous ions. To ensure homogeneous dispersion, the as-prepared sample was kept under ultrasonic treatment for about 30 minutes; thereafter, the sample was allowed to dry in an oven at 90°C for 36 hours to eliminate remaining impurities.

2.3. Measurements

The crystal structure of the exfoliated graphene was analyzed using a Rigaku MiniFlex 600 X-ray diffractometer. The diffraction patterns were recorded in the 2θ range of 10°-80° at a scanning rate of 5° min^{-1}, employing CuKα radiation (λ = 1.5418 Å). Raman spectra were recorded using an InVia Renishaw Raman spectrometer with 532 nm laser excitation. The morphological characteristics of the powdered sample were examined with a JEOL JSM6360A scanning electron microscope (SEM) at an accelerating voltage of 20 kV under high-vacuum conditions. The absorption spectrum of the exfoliated graphene was obtained using a Systronics spectrophotometer 117. A TEM image was obtained using a JEOL JEM-1400 instrument operated at an accelerated voltage in the range of 80-120 kV. The absorption spectra of exfoliated graphene were obtained using a Model 117 μ-controller-based UV–Visible spectrophotometer manufactured by Systronics, India. The instrument was equipped with a tungsten-halogen lamp (320–1100 nm) and a deuterium lamp (200–340 nm) as radiation sources.

3. Results and discussion

X-ray diffraction was used to examine the structural transformation of graphite during electrochemical exfoliation. A comparison of the diffraction patterns for the starting graphite and the exfoliated graphene is presented in Figure 2. As expected, both samples show a dominant peak at 2θ ~ 26.4°, assigned to the (002) plane of layered sp^2-bonded carbon [19]. For graphite, this peak appears sharp and highly intense, reflecting its well- ordered crystalline stacking and strong interlayer coherence. Furthermore, the exfoliated graphene displays the same (002) reflection with reduced intensity and slight peak broadening. This indicates a loss of long-range order along the c-axis, caused by the separation of graphene layers during electrochemical delamination. The disruption of van der Waals attractions between layers results in thinner stacks and the formation of few-layer to some multi-layer graphene sheets. A very weak peak also appears near 2θ ~ 54.4°, corresponding to the (004) plane [20]. Its significantly lower intensity in the exfoliation product suggests that only a small portion of multi-layer regions remains. Importantly, no additional peaks were detected, confirming that the exfoliation process did not introduce new crystalline phases or impurities.

The average crystallite size was determined from the (002) diffraction peak using the Debye-Scherrer relation: $D_{002}=0.89\lambda/\beta \cdot \cos\theta$, where β represents the full width at half maximum (FWHM) of the corresponding reflection.

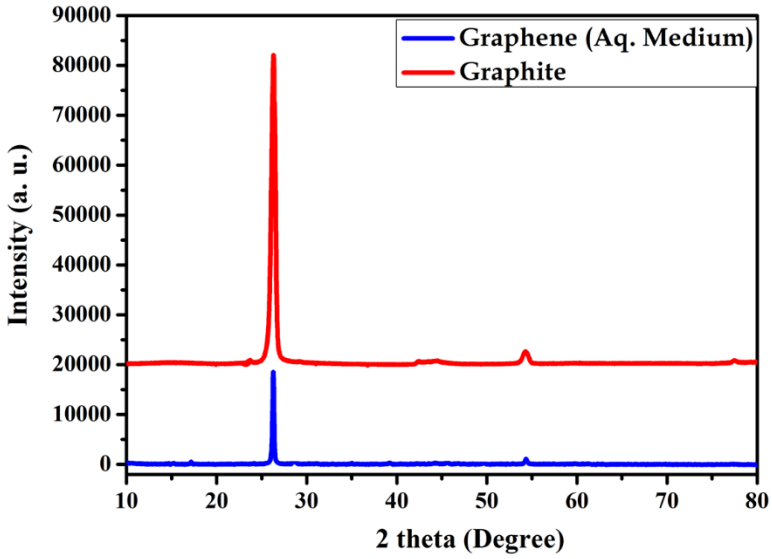

Figure 2. XRD profiles of graphite and exfoliated graphene showing reduced (002) peak intensity, confirming successful layer separation.

The graphite electrode displays a well-defined (002) reflection associated with an interlayer spacing of approx. 0.338 nm and a comparatively large crystallite dimension of 59.37 nm, indicative of a highly ordered structure with extensive stacking of graphitic layers. Moreover, the electrochemically exfoliated graphene sample exhibits a slight increase in interlayer spacing (~0.339 nm), along with a discernible broadening of the diffraction feature, corresponding to a reduction in crystallite size to ~29 nm. Such changes reflect a decrease in structural coherence along the c-axis, suggesting that the long-range stacking order has been partially disrupted. The observed increase in interlayer separation further implies a weakening of interlayer interactions, which may arise from ion intercalation and structural modification introduced during the exfoliation process.

To examine the internal structure of our as-synthesized graphene sample, we conducted detailed Raman spectroscopy studies at room temperature, recorded at a 532 nm wavelength. The measurement conditions were carefully controlled, employing a low power (0.1 mW) and short exposure time (0.5 s) to minimize any thermal effects. The frequency of each vibrational mode can be determined by fitting, as illustrated in Figure 3. Three characteristic Raman peaks were identified corresponding to the D-band at 1351 cm^{-1}, the G-band at 1593 cm^{-1}, and the 2D-band at 2702 cm^{-1} [21, 22]. A detailed examination of these bands unlocks crucial and highly informative insights. G-peak at 1593 cm^{-1} corresponds to the presence of planar vibrational sp^2-hybridized carbon atoms and is attributed to the in-plane stretching vibrations with the graphene framework.

The G-band, stemming from the E_{2g} in-plane vibrational modes of sp^2 carbon atoms at the Γ-point, encompasses both LO and TO phonons; it serves as a definitive spectral feature of graphene and other sp^2-bonded carbon material [22]. This band is resonant, which results in its intensity being significantly higher under normal conditions, signifying a reduced number of stacked graphene layers. The observed band spot is closely aligned with the calculated values of these band locations. Attributed to the ring-breathing mode of sp^2-hybridized carbon atoms, the D-band appears when symmetry is broken, typically near the edges or in regions with defects within the graphene lattice [23]. However, its intensity increases linearly with the defect density, thus serving as a diagnostic tool for quantifying disorder within the graphene lattice.

Representing the second-order overtone of the D-band, the 2D-band arises from a two-phonon process involving TO phonons near the K-point. Its activation is governed by TRRS, which enhances its intensity even in defect-free graphene, making it a key feature for

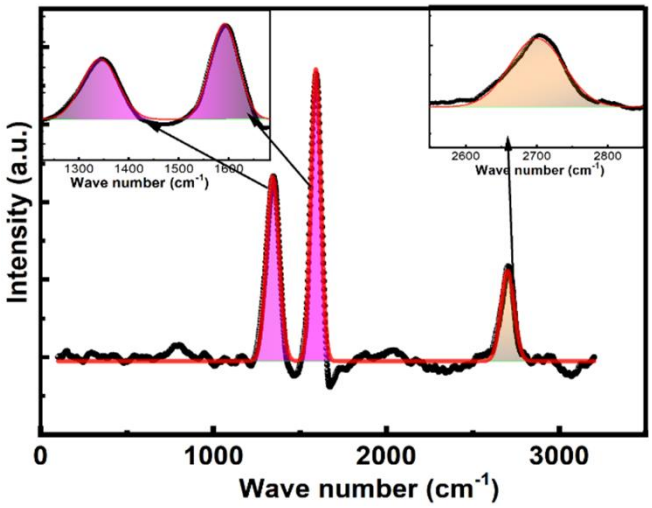

Figure 3. Raman spectra of as-produced exfoliated graphene, red line shows the Lorentzian fitting, and expanded peaks (insets).

evaluating the number of graphene layers. It exhibits significant dispersion with excitation energy, attributed to a Kohn anomaly at the K-point, and unlike the D-band, it does not require activation by the presence of defects. Consequently, the 2D-band exhibits strong intensity in graphene, independent of the D-band, and does not signify the presence of defects within the lattice. The 2D-band is frequently used to estimate graphene layer thickness. The integrated intensity ratio of 2D- and G-band (I_{2D}/I_G) serves as a reliable indicator for determining the number of graphene layers. The value of I_{2D}/I_G obtained was 0.42, in this case, indicating the successful synthesis of multi-layer graphene structures. This ratio aligns with the degree of sp^2-hybridization, with values ≥ 2, 1-2, and < 1, respectively corresponding to single-, few-, and multi-layered graphene [24, 25].

Further, it is important to note that the level of disorder in graphene can be analyzed through the ratio of the intensities of D- to G-peaks, i.e., I_D/I_G. In this study, we obtained a defect density of 0.63, indicating that our sample has fewer structural disruptions, which can enhance certain properties, such as energy storage. Defects can enhance the surface area and reactivity of graphene. In some cases, defects can also arise from surface-bound functional groups on graphene during exfoliation. The sharp edge of D-band and its high intensity indicate some level of chemical modification or functionalisation. The edge of graphene is a distinct defect that activates the D-peak in Raman spectra. The ratio of intensity of D- to G-band, i.e., I_D/I_G, is frequently used to estimate the crystallite size (L_a), from the Tuinstra-Koenig relation [26]:

$$L_a = 2.4 \times 10^{-10} \times \lambda^4 \times I_G/I_D \text{ nm} \quad (1)$$

where λ = 532 nm, and the observed L_a value is approximately 30.4 nm. This value indicates a moderate level of disorder and edge-induced defects, typically for graphene produced via electrochemical exfoliation, while still retaining relatively large sp^2 domains. Such a size is favorable for energy storage and sensor applications.

To assess the elemental distribution, EDS analysis was undertaken. The compositional analysis of as-synthesized electrochemically exfoliated graphene is presented in Figure 4(a). The atomic% and weight% are provided in Table 2. The EDS spectrum confirms the presence of carbon and oxygen. The embedded image within Figure 4(a), inset, highlights the typical SEM micrograph of as-produced electrochemically exfoliated graphene in aqueous medium. The analysis confirmed the formation of graphene, which exhibits a rough surface with wrinkles, crumples, and planar distortion, which is a key characteristic feature of graphene [27, 28].

Table 1. Spectral Characteristics of as-synthesized exfoliated graphene via Raman Spectra

Specimen	2D-band (cm^{-1})	G-band (cm^{-1})	D-band (cm^{-1})	I_D/I_G	I_{2D}/I_G	L_a (nm)
Exfoliated Graphene	2702	1593	1351	0.63	0.42	30.4

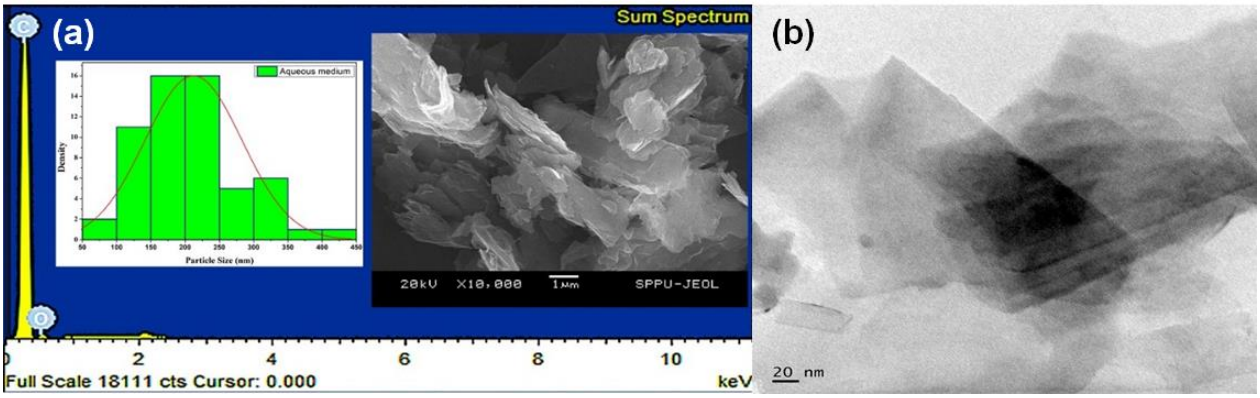

Figure 4. (a) EDS, scanning electron images (inset) and particle size distribution (inset), and (b) TEM image of as-produced electrochemically exfoliated graphene.

The roughened surface results from mechanical distortions introduced throughout the exfoliation process, coupled with partial reassembly of graphene nanosheets. Interaction with strongly nucleophilic ions facilitates the delamination of graphene sheets, effectively reducing the number of layers within the graphene sheets. Raman spectra stipulations further confirmed through SEM observation, i.e., the presence of multi-layered graphene, especially N-layered graphene, but the high intensity and broad area of the 2D-peak suggests that the N is quite small (the number of layers is quite low). The SEM images reveal a multilayered structure of graphene, with some traces of few-layered graphene. The stack arrangement of graphene layers is distinctly visible in the SEM image. It is important to distinguish multi-layered graphene from graphite, as the graphite's intrinsic layer-to-layer separation is significantly larger (0.335 nm) compared to that of N-layered graphene. A size distribution histogram (Figure 4a, inset), based on SEM imaging of the electrochemically exfoliated graphene flakes, shows the mean flake size of 225 nm. In contrast, the flakes demonstrate a markedly increased lateral size relative to those produced through conventional shear or liquid-phase exfoliation in aqueous medium.

Further, transmission electron microscopy (TEM) was employed to investigate the microstructural features, layer thickness, and exfoliation quality of the electrochemically exfoliated graphene synthesized in an aqueous medium. TEM is particularly effective for graphene-based materials, as it provides direct visualization of sheet morphology, transparency, folding behavior, and relative thickness variations at the nanoscale [29, 30]. The TEM micrograph (Figure 4b) reveals the presence of large-area, thin, sheet-like structures with irregular lateral dimensions, confirming the successful delamination of bulk graphite into graphene sheets.

Table 2. Atomic % and weight % of electrochemically exfoliated graphene

Element	Weight (%)	Atomic (%)
C	95.04	96.23
O	4.96	3.77

The high degree of electron transparency observed across extensive regions of the sample is indicative of few-layer graphene with some multi-layered regions, as ultrathin graphene allows significant transmission compared to thicker graphite domains [31]. Distinct contrast variation is evident within individual graphene flakes. Lighter regions correspond to few-layer graphene (approximately 2-4 layers), while comparatively darker regions indicate locally stacked multilayered graphene (approximately 5-7 layers). Such contrast-dependent thickness variation is a well-established criterion for qualitative layer estimation in plan-view TEM imaging of graphene materials. Importantly, no highly opaque or bulk graphite-like regions are observed, demonstrating effective exfoliation and minimal presence of unexfoliated graphene.

The graphene sheets exhibit wrinkled and folded morphologies, particularly near the edges. These features arise from the intrinsic flexibility of two-dimensional graphene sheets and from strain induced during exfoliation and solvent evaporation during TEM sample preparation. Besides, the edges of the graphene

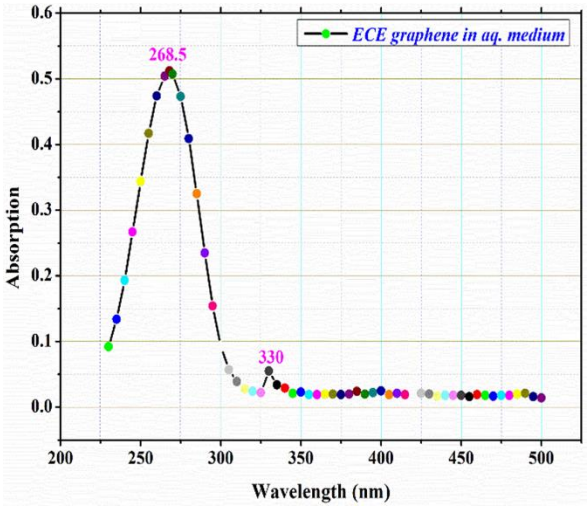

Figure 5. UV-Visible spectrum of as-synthesized graphene.

sheets appear well-defined and sharp, rather than amorphous or severely damaged, suggesting that the electrochemical exfoliation process preserved the structural integrity of the graphene lattice. The absence of amorphous carbon deposits or particulate contaminants indicates high purity of synthesized graphene, reflecting the advantage of using a mild aqueous electrolyte system during exfoliation. The coexistence of few-layer and limited multi-layered regions suggests a non-uniform but efficient exfoliation process, which is commonly reported for electrochemical exfoliation methods.

Partial restacking of graphene sheets is likely to occur during post-exfoliation washing, filtration, and drying steps; however, the dominance of few-layer regions confirms the effectiveness of the electrochemical approach in achieving substantial graphite delamination. These TEM observations are in strong agreement with Raman spectroscopic analysis. Also, the moderate I_D/I_G ratio of 0.63 indicates the presence of edge-related and exfoliation-induced defects rather than extensive basal-plane disorder, which is consistent with the well-preserved lattice observed in TEM. Further, the I_{2D}/I_G ratio of 0.42 and the broadened 2D band further support the presence of few-layer graphene rather than monolayer graphene, corroborating the TEM-based layer estimation. The Raman-derived in-plane crystallite size of approx. 30.4 nm aligns well with the large lateral graphene domains observed in TEM images.

From an application perspective, the observed microstructure is highly favorable. Few-layer graphene regions provide high surface area and excellent electrical conductivity, while occasional multilayer stacking contributes to mechanical stability and barrier properties. This combination is particularly advantageous for electrochemical energy storage and anticorrosion applications, where rapid charge transport and impermeability to aggressive species are essential.

The as-synthesized electrochemically exfoliated graphene was analyzed using UV-vis. spectroscopy (Figure 5), revealing its characteristic absorption peak. It involves the absorption of light within a specific wavelength range of 200-800 nm. The UV-vis. spectrum displays a prominent absorption peak at 268.5 nm; this feature arises due to the electronic transition from the π (bonding orbital) to some agitated π* (anti-bonding) level within conjugated C=C bonds, indicative of the graphitic sp^2 domain [29]. The sharp and intense peak suggests the retention of conjugated domains and highlights the efficiency of the exfoliation process. Besides, a peak with very low intensity near 330 nm is noted; this feature is ascribed to n to π* shifts arising from residual oxygen functional groups, likely localized at the edges or functional sites introduced during exfoliation, which is also evident from SEM and EDS data [30].

The relatively low intensity of spectra at 330 nm suggests minimal oxidation, further supporting the intrinsic structural integrity of as-synthesized graphene sheets. Also, compared to graphene, graphene oxide (GO) reveals a notable absorption peak at 230 nm due to π-π* electronic transition in the conjugated C=C

framework, accompanied by a weaker band near 303 nm associated with the n-π* electronic transition of carbonyl (C=O) functionalities [30, 32]. For reduced graphene oxide (rGO), the absorption peak undergoes a redshift to around 255 nm, reflecting a reduction of the oxygen-based functional groups and the restoration of conjugated aromatic domains. This redshift indicates that the electron excitation occurs to a higher energy band with a slightly lower energy [20].

4. Conclusions

The current study demonstrates the successful synthesis of graphene from graphite through the electrochemical exfoliation technique in an aqueous medium. This method presents several advantages, including its environmentally friendly, one-pot process, operational simplicity, and the use of no harsh or toxic chemical reagents. Comprehensive structural and spectroscopic characterization confirms the successful formation of graphene with preserved graphitic features. XRD analysis reveals a reduction in the (002) peak intensity along with slight peak broadening, indicating exfoliation and partial loss of long-range stacking order. Raman spectroscopy shows characteristics D, G, and 2D bands with an I_D/I_G ratio of ~0.63, suggesting a moderate defect density primarily associated with edge sites and exfoliation induced structrul distortions. The I_{2D}/I_G ratio further supports the formation of multi-layered graphene, which is consistent with TEM observation indicating 3-6 stacked layers. SEM analysis reveals crumpled, sheet-like morphology with lateral flake dimensions on the order of ~225 nm, while EDS confirms a high carbon content (~95–96%), indicating limited oxidation. UV-Visible spectroscopy exhibits a prominent adsorption peak at ~268.5 nm with a weak shoulder near ~330 nm, characteristic of π–π* transitions and minor residual functional groups.

Overall, the developed method provides a viable pathway for producing good-quality graphene with controlled defect density and minimal chemical complexity. The combination of moderate structural disorder and preserved sp^2 domains is advantageous for applications requiring active surface sites alongside good electrical conductivity. Further work should focus on quantitative yield optimization, detailed surface chemistry analysis, and controlled tuning of layer number and defect density to further enhance material performance for targeted applications such as energy storage and functional coating.

Acknowledgments

PRH is admirably grateful for the financial support of the University Grants Commission, New Delhi as SRF. Authors are thankful to the Central Instrumentation Facility, Department of Physics, SBP Pune University, Pune, for providing SEM, TEM and Raman spectroscopy data.

Conflict of Interest

The authors declare no conflict of interest.

References

1. A.K. Geim and K.S. Novoselov. The rise of graphene. *Nature Materials*, **2007**, *6*, 183.
2. X. Jiang, et al. An easy one-step electrosynthesis of graphene/polyaniline composites and electrochemical capacitor. *Carbon*, **2014**, *67*, 662.
3. M.C. Lemme, et al. A Graphene Field-Effect Device. *IEEE Electron Device Letters*, **2007**, *28*, 282.
4. S. Stankovich, et al. Graphene-based composite materials. *Nature*, **2006**, *442*, 282.
5. M.D. Stoller, et al. Graphene-Based Ultracapacitors. *Nano Letters*, **2008**, *8*, 3498.
6. Y. Zhu, et al. Graphene and Graphene Oxide: Synthesis, Properties, and Applications. *Advanced Materials*, **2010**, *22*, 3906.
7. K.S. Novoselov, et al. Electric Field Effect in Atomically Thin Carbon Films. *Science*, **2004**, *306*, 666.
8. A.N. Obraztsov, et al. Chemical vapor deposition of thin graphite films of nanometer thickness. *Carbon*, **2007**, *45*, 2017.
9. K.S. Kim, et al. Large-scale pattern growth of graphene films for stretchable transparent electrodes. *Nature*, **2009**, *457*, 706.
10. T.A. Land, et al. STM investigation of single layer graphite structures produced on Pt(111) by hydrocarbon decomposition. *Surface Science*, **1992**, *264*, 261.
11. R. Ruoff. Calling all chemists. *Nature Nanotechnology*, **2008**, *3*, 10.

12. W.S. Hummers and R.E. Offeman. Preparation of Graphitic Oxide. *Journal of the American Chemical Society*, **1958**, *80*, 1339.

13. X. Lu, et al. Controllable Synthesis of 2D Materials by Electrochemical Exfoliation for Energy Storage and Conversion Application. *Small*, **2022**, *19*, 2206702.

14. Y. Zhang, et al. Ultrafast alternating-current exfoliation toward large-scale synthesis of graphene and its application for flexible supercapacitors. *Journal of Colloid and Interface Science*, **2024**, *654*, 246.

15. P. Tripathi, et al. High yield synthesis of electrolyte heating assisted electrochemically exfoliated graphene for electromagnetic interference shielding applications. *RSC Advances*, **2015**, *5*, 19074.

16. M. Zhou, et al. Few-layer graphene obtained by electrochemical exfoliation of graphite cathode. *Chemical Physics Letters*, **2013**, *572*, 61.

17. C.J. Raj, et al. Sonoelectrochemical exfoliation of graphene in various electrolytic environments and their structural and electrochemical properties. *Carbon*, **2021**, *184*, 266.

18. X. Zhao, et al. Electrochemical exfoliation of graphene as an anode material for ultra-long cycle lithium ion batteries. *Journal of Physics and Chemistry of Solids*, **2020**, *139*, 109301.

19. Y.Z.N. Htwe, et al. Effect of electrolytes and sonication times on the formation of graphene using an electrochemical exfoliation process. *Applied Surface Science*, **2019**, *469*, 951.

20. F.T. Thema, et al. Synthesis and Characterization of Graphene Thin Films by Chemical Reduction of Exfoliated and Intercalated Graphite Oxide. *Journal of Chemistry*, **2012**, *2013*, 150536.

21. A. Eckmann, et al. Probing the Nature of Defects in Graphene by Raman Spectroscopy. *Nano Letters*, **2012**, *12*, 3925.

22. K.S. Rao, et al. Role of Peroxide Ions in Formation of Graphene Nanosheets by Electrochemical Exfoliation of Graphite. *Scientific Reports*, **2014**, *4*, 4237.

23. A.C. Ferrari, et al. Raman Spectrum of Graphene and Graphene Layers. *Physical Review Letters*, **2006**, *97*, 187401.

24. B. Subramanya and D.K. Bhat. Novel one-pot green synthesis of graphene in aqueous medium under microwave irradiation using a regenerative catalyst and the study of its electrochemical properties. *New Journal of Chemistry*, **2015**, *39*, 420.

25. C. Shan, et al. Facile Synthesis of a Large Quantity of Graphene by Chemical Vapor Deposition: an Advanced Catalyst Carrier. *Advanced Materials*, **2012**, *24*, 2491.

26. R. Sharma, N. Chadha, and P. Saini. Determination of defect density, crystallite size and number of graphene layers in graphene analogues using X-ray diffraction and Raman spectroscopy. *Indian Journal of Pure & Applied Physics*, **2017**, *55*, 625.

27. J. Nishijo, et al. Synthesis, structures and magnetic properties of carbon-encapsulated nanoparticles via thermal decomposition of metal acetylide. *Carbon*, **2006**, *44*, 2943.

28. T.C. Achee, et al. High-yield scalable graphene nanosheet production from compressed graphite using electrochemical exfoliation. *Scientific Reports*, **2018**, *8*, 14525.

29. K. Anurag and S.R. Kumar. Scalable preparation of high-quality graphene by electrochemical exfoliation: effect of hydrogen peroxide addition. *Bulletin of Materials Science*, **2023**, *46*, 42.

30. M. El Achaby, et al. Piezoelectric β-polymorph formation and properties enhancement in graphene oxide – PVDF nanocomposite films. *Applied Surface Science*, **2012**, *258*, 7668.

31. S.J. Pennycook. Transmission Electron Microscopy: A Textbook for Materials Science, Second Edition. David B. Williams and C. Barry Carter. Springer, New York, 2009, 932 pages. ISBN 978-0-387-76500-6 (Hardcover), ISBN 978-0-387-76502-0 (Softcover). *Microscopy and Microanalysis*, **2010**, *16*, 111.

32. S. Thakur and N. Karak. Green reduction of graphene oxide by aqueous phytoextracts. *Carbon*, **2012**, *50*, 5331.